MATHEMATICAL MODEL OF AUTOMATIC FIRING SYSTEM OF GAS-OPERATED MACHINE GUN

UDC:623.442.4:519.673
Original scientific paper https://doi.org/10.18485/aeletters.2023.8.3.1

Vo Van Bien[1], Nguyen Duy Phon[1*], Nguyen Minh Phu[1]

[1]The Faculty of Special Equipments, Le Quy Don Technical University, Hanoi City, 100000, Vietnam

Abstract:
This paper mentions a new approach to accurately and fully describe the mathematical model of the automatic firing system of gas-operated machine guns. The mathematical model is established based on Lagrange's equations of the second kind. A numerical method was used to solve the research problem. The automatic firing system of the PKMS machine gun (of Russian origin) was selected for calculation and testing. After the research model is calculated, a comparison is made between the theoretical calculation results and the experimental results to verify the mathematical model. The comparison results between the calculation from the theoretical model and the results obtained from the experiment show that the mathematical model is suitable and reliable, the maximum velocity error of the bolt carrier is only 6.53%. The results obtained from this study are the basis for evaluating the working ability of the automatic firing system. This is also a reliable theoretical basis for designers to optimize the structure for automatic firing systems of gas-operated automatic weapons.

ARTICLE HISTORY
Received: 27 March 2023
Revised: 21 July 2023
Accepted: 7 August 2023
Published: 30 September 2023

KEYWORDS
The automatic firing system,
the PKMS machine gun,
gas-operated weapons,
Lagrange's equation

1. INTRODUCTION

The automatic firing system is an important part of automatic weapons. This system has a complex structure and works with high precision requirements. So its kinetic properties directly affect the stability of the entire weapon system when firing. The energy for the automatic firing system to work is generated by several methods. In particular, the automatic firing system using combustible gas energy is mainly used. Based on the principle of using the energy of the combustible gas, the automatic firing system of the weapon is divided into three types: The automatic firing system works on the principle of blow-back weapons, the automatic firing system works on the principle of the recoil – operated weapons and the automatic firing system works on the principle of gas-operated, [1-11]. Automatic weapons operating on the principle of gas-operated are commonly used because it has a simple structure, the structure of the air chamber is capable of adjusting the level of effect of the combustible gas on the piston. Structural diagrams of the movable piston and fixed cylinder automatic weapons are shown in Fig. 1, [5, 8].

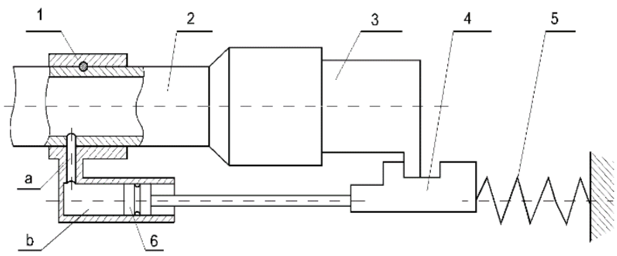

Fig. 1. Schematic of gas–operated weapons [5], (1. Gas block; 2. Barrel; 3. Bolt; 4. The bolt carrier; 5. Return spring; 6. Piston; a. Gas port; b. Gas cylinder)

For a gas-operated weapon, part of the combustible gas is extracted through the barrel to operate the automatic firing system. This system is used in small arms with a normal rate of fire and in weapons with a high rate of fire when fired. As the bullet passes through the gas port, the gases enter the gas chamber, where they transmit a force to the

*CONTACT: N.D. Phon, e-mail: phonnduy@gmail.com

piston. This force is transmitted to the automatic firing system (usually to the bolt carrier). The flow of gas entering the gas chamber during firing depends on the cross-sectional area of the gas port hole. This gas flow is important because it affects the gas pressure in the air chamber, which also influences the weapon's operation, [2, 6, 7].

The problem of automatic firing system dynamics is one of the important problems in the design, exploitation, and use of automatic weapons. Determining this problem is also different for each specific automatic gun. The result of the dynamics problem of the automatic firing system is to determine the rate of fire, the law of displacement of the base mechanism (usually the bolt carrier), the force and the moment acting on the gun, etc. This calculation result is also the input data to solve the problem of the weapon system's stability when firing and to evaluate the superiority of automatic guns.

For the above reasons, there have been a large number of documents, studies, and simulation tools that have been used by previous researchers to research, design and optimize automatic firing systems. Some of the most notable documents are [12-23]. However, the problem of calculating the dynamics of automatic firing systems of gas-operated weapons has not been studied methodically and fully. Some studies consider the force exerted by the combustible gas on the piston of the automatic firing system to be one-direction, while others consider only the process of gas flowing from the barrel into the gas chamber, refer to [12]. Experimental and semi-empirical methods used to determine the combustion gas pressure in the gas chamber are presented in the [13] document. These methods are easy to use and simple in data processing, but the accuracy is not high. In recent years, the method of numerical integration has been widely used by many researchers and has obtained many remarkable achievements, [14-17]. Besides, the calculation of fluid dynamics (CFD) has been interesting and applied by many researchers to study and analyze the gas flow through the gas port hole, [18-21]. However, these studies have not completely solved the dynamics of the automatic firing system. Some studies have only solved this problem in the backward movement stage of the bolt carrier, [14, 15, 17, 20-21]. Notably, the experimental method has also been used to determine the dynamic parameters of the automatic firing system, refer to [22, 23]. However, this method requires high experimental costs and does not fully reflect the physical nature of the shooting phenomenon. Therefore, a detailed study on the automatic firing system of automatic gas-operated weapons is very necessary and has high practical value. This study focuses on building a mathematical model with the conditions closest to the actual model. The experimental study was conducted with modern high-precision measuring devices.

2. MATERIALS AND METHODS

The article presented a detailed and complete study of the dynamics of the automatic firing system of gas-operated automatic weapons. The mathematical model of the automatic firing system is established based on Lagrange's equations of the second kind, [3, 24-25]. This problem is solved by numerical method on Matlab software. The automatic firing system of the PKMS machine gun (of Russia) was selected for calculation and testing in this study, Fig. 2. The calculated results are compared with the corresponding experimental data to verify the reliability of the theoretical model. In the experimental part of this study, we used a non-contact measurement method to determine the displacement of the automatic firing system's base mechanism (the bolt carrier). High-speed cameras have been used in this method for highly accurate results. This measurement method does not affect the weapon system during test firing. After processing, the measured results are used to verify the established mathematical model. The dynamic model in this paper can be used to calculate the optimal design of the automatic firing system of gas-operated automatic weapons.

Fig. 2. The PKMS machine gun

3. PROBLEM FORMULATION

3.1. Model of the gas-operated weapon

The problem of dynamics of the automatic firing system of gas-operated weapons is a combination of three problems: the interior ballistic problem, the thermodynamics of the gas chamber, and the motion problem of the automatic firing system. The problems of the interior ballistic problem and the problem of gas chamber thermodynamics have been detailed in the documents [3, 5, 16]. Therefore, the main content of this study focuses on solving the motion problem of the automatic firing system when firing.

The dynamic model of the automatic firing system of an automatic gas-operated weapon is established based on the following assumptions, [1]:

- All parts of the automatic firing system are absolutely solid except for the return spring;
- The mass of solids does not change, it is replaced by a concentrated mass located at the center of gravity of the object;
- The effect of the gap between dynamic joints is ignored;
- The article focuses on studying the movement of the base mechanisms (in particular, of the bolt carrier) without solving the problem of stability and oscillation of the gun when firing;
- Neglect rotation, swing, and vertical movement of the base mechanism. Studying only the bolt carrier's movement along the barrel's axis.

The automatic firing system of a gas-extracting automatic weapon consists of a base mechanism (usually a bolt carrier) of mass m_0 and working mechanisms of mass m_i (whose motion depends on the movement of the basic mechanism), [2-9]. Angle α_i represents the angular deviation of the direction of motion of the i-th working link with the base link. For the gas-operated automatic weapon, two main working mechanisms have been considered that greatly affect the movement of the base mechanism, which are the bolt (m_1) and the feed mechanism (m_2). The physical model of the automatic firing system is shown in Fig. 3.

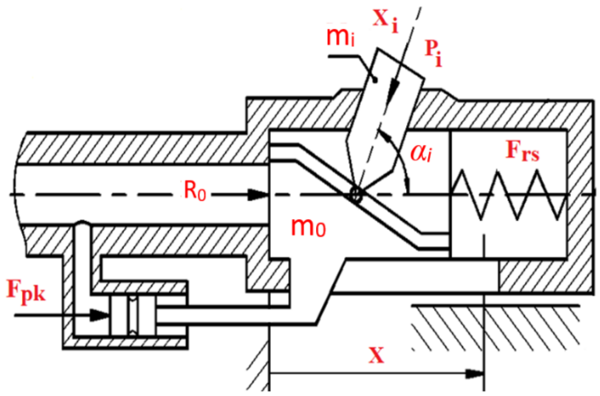

Fig. 3. The physical model of the automatic firing system

The differential equations of motion of the automatic firing system can be obtained by the following methods: using Dalambe's principle for each mechanism, a method using Newton's 2nd law, and using Lagrange's equations of the second kind. Because the gas-operating automatic firing system has many kinetic constraints, Lagrange's equations of the second kind were used in this study [24, 25]. The general Lagrange equation of the second kind is expressed by the following equation:

$$\frac{d}{dt}\left(\frac{\partial T}{\partial \dot{q}_j}\right) - \frac{\partial T}{\partial q_j} + \frac{\partial \Pi}{\partial q_j} = Q_j (j = 1,2,\dots). \quad (1)$$

Where: T – the total kinetic energy of the whole system; Π – the potential energy of the system; q_j – the independent generalized coordinate; Q_j – the generalized force; j - number of degrees of freedom.

Corresponding to the physical model of the automatic firing system in Fig. 3, the generalized coordinates in the system are q_1 = x (displacement of base mechanism relative to the gun body), q_i = x_i (displacement of working mechanism relative to the gun body). Where $q_1=x$ is the independent generalized coordinate, $q_i=x_i$ is the dependent generalized coordinate.

The expression for the kinetic energy of the system is determined by the following equation, [24]:

$$T = \frac{m_0 V^2}{2} + \sum_{i=1}^{n} \frac{m_i {V_i}^2}{2}. \quad (2)$$

Where, V – velocity of base mechanism relative to the gun body; V_i – velocity of the i-th working mechanism relative to the gun body; n – number of working mechanisms.

The absolute velocities of the bodies in the mechanical system are expressed through generalized coordinates as follows:

$$V^2 = \dot{x}^2.$$
$$V_i^2 = \dot{x}_i^2 = {k_i}^2 \dot{x}^2. \quad (3)$$

Where k_i – is the transmission ratio between the base mechanism and the i-th working mechanism. k_i - function of the displacement of the base mechanism, $k_i = f(x)$.

Substituting expression (3) into equation (2), the expression for the kinetic energy of the mechanical system is determined as follows:

$$T = \frac{1}{2}\left(m_0 + \sum_{i-1}^{n} {k_i}^2 m_i\right)\dot{x}^2. \quad (4)$$

The expression for determining partial derivatives is as follows:

$$\frac{\partial T}{\partial x} = \dot{x}^2 \sum_{i=1}^{n} k_i m_i \frac{\partial k_i}{\partial x}.$$
$$\frac{\partial T}{\partial \dot{x}} = \left(m_0 + \sum_{i=1}^{n} {k_i}^2 m_i\right)\dot{x}. \quad (5)$$
$$\frac{d}{dt}\left(\frac{\partial T}{\partial \dot{x}}\right) = \left(m_0 + \sum_{i=1}^{n} {k_i}^2 m_i\right)\ddot{x} + 2\dot{x}^2 \sum_{i=1}^{n} \frac{\partial k_i}{\partial x} m_i k_i.$$

The potential energy of the system is determined:

$$\Pi = \Pi_0 x + \frac{1}{2} c_0 x^2. \quad (6)$$

Where, Π_0 – is the initial compression force of the return spring, and c_0 – is the stiffness of the return spring.

Differentiate Equation (6) concerning the variable x:

$$\frac{\partial \Pi}{\partial x} = \Pi_0 + c_0 x. \quad (7)$$

Expression for determining the generalized force:

$$Q_1 = P_0 - \sum_{i=1}^{n} k_i P_i - \left(\sum_{i=1}^{n} F_{0x} + \sum_{i=1}^{n} k_i F_i\right). \quad (8)$$

Where, P_0 - external force acting on the base mechanism; P_i - external force acting on the i-th working mechanism; F_i - friction force between the i-th working mechanism and the base mechanism; F_{0i} - frictional force acting on the base mechanism at the position associated with the i-th working mechanism.

On the other hand, Lagrange's equations of the second kind are only applicable to a system with an ideal connection, in practice there is always a dissipation of energy by the frictional force between the base and the working mechanism. Therefore, to account for this loss, the transmission efficiency η_i between the base mechanism and the working mechanism is determined as follows:

$$\eta_i = \frac{R_i}{R_o} k_i. \quad (9)$$

Where, Ro - force acting on the base mechanism; R_i - useful resistance forces acting on the working mechanism.

The expression is determined according to Fig. 4:

$$R_o = R_{ax} + F_{0x}.$$
$$R_i = R_b - F_i. \quad (10)$$

Where, R_{ax}, R_b - projection of the reactions R on the directions of motion; F_{0x}, F_i - projection of friction force on the directions of motion.

Useful resistance on the i-th working mechanism:

$$R_i = m_i \frac{d\dot{x}_i}{dt} + P_i. \quad (11)$$

With n working mechanism:

$$\sum_{i=1}^{n} R_0 = \sum_{i=1}^{n} R_{ax} + \sum_{i=1}^{n} F_{0x}. \quad (12)$$

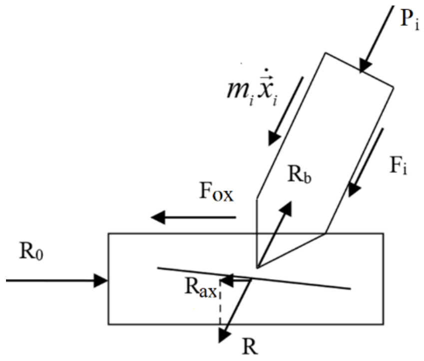

Fig. 4. Forces acting on the base and working mechanism

Substituting equations (9) and (11) into equation (12), we get:

$$\sum_{i=1}^{n} \frac{k_i}{\eta_i}\left(m_i \frac{d\dot{x}_i}{dt} + P_i\right) = \sum_{i=1}^{n} R_{ax} + \sum_{i=1}^{n} F_{0x}. \quad (13)$$

After the transformation:

$$\sum_{i=1}^{n} F_{0x} + \sum_{i=1}^{n} k_i F_i = \sum_{i=1}^{n} k_i \left(\frac{1}{\eta_i} - 1\right)\left(m_i \frac{d\dot{x}_i}{dt} + P_i\right). \quad (14)$$

The substitution of frictional forces by transmission efficiency is shown in expression (14).

On the other hand, the gear ratio expression:

$$\dot{x}_i = k_i \dot{x}. \quad (15)$$

Differentiate both in terms of equation (15):

$$\frac{d\dot{x}_i}{dt} = \dot{x}^2 \frac{dk_i}{dx} + k_i \ddot{x}. \quad (16)$$

Substituting expressions (14), and (16) into expression (8), the expression for determining the generalized force is as follows:

$$Q_1 = P_0 - \sum_{i=1}^{n} \frac{k_i}{\eta_i} P_i - \sum_{i=1}^{n} k_i m_i \left(\frac{1}{\eta_i} - 1\right)\left(\dot{x}^2 \frac{dk_i}{dx} + k_i \ddot{x}\right). \quad (17)$$

Substituting equations (5), (7), and (17) into equation (1), we get the differential equation of motion of the base mechanism with the following form:

$$M_{11}\ddot{x} + M_{12}\dot{x}^2 + c_0 x = P_1. \quad (18)$$

Where:

$$M_{11} = m_0 + \sum_{i=1}^{n} \frac{{k_i}^2}{\eta_i} m_i.$$
$$M_{12} = \sum_{i=1}^{n} \frac{k_i}{\eta_i} m_i \frac{dk_i}{dx}. \quad (19)$$
$$P_1 = P_0 - \Pi_0 - \sum_{i=1}^{n} \frac{k_i}{\eta_i} P_i.$$

If the automatic firing system has n reciprocating mechanisms and q rotary actuators then the equation (19) is redefined as:

$$M_{11} = m_0 + \sum_{i=1}^{n} \frac{{k_i}^2}{\eta_i} m_i + \sum_{s=1}^{q} \frac{{k_s}^2}{\eta_s} I_s \cos\beta_s \sin\gamma_s .$$
$$M_{12} = \sum_{i=1}^{n} \frac{k_i}{\eta_i} m_i \frac{dk_i}{dx} + \sum_{s=1}^{q} \frac{k_s}{\eta_s} I_s \frac{dk_s}{dx} \cos\beta_s \sin\gamma_s . \quad (20)$$
$$P_1 = P_0 - \Pi_0 - \sum_{i=1}^{n} \frac{k_i}{\eta_i} P_i - \sum_{s=1}^{q} \frac{k_s}{\eta_s} L_s .$$

Where: k_s, η_s - transmission ratio and rotational efficiency between the base mechanism and the s-th working mechanism; I_s - moment of inertia of the s-th working mechanism; r_s - replacement radius; L_s - resistance torque acting on the s-th working mechanism; β_s - the angle of inclination of the axis of rotation of the s-th working mechanism with the direction of motion of the base mechanism; γ_s - the angle of inclination of the radius of inertia of the s-th working mechanism with its axis of rotation.

Equation (18) can be rewritten as:

$$\begin{cases} \dot{x} = V. \\ \dot{V} = \frac{1}{M_{11}} \left[P_1 - M_{12} V^2 - c_0 x \right]. \end{cases} \quad (21)$$

3.2. Main forces acting on the mechanical system

The main forces acting on the bolt carrier are shown in Figs. 5 and 6. Fig. 5 shows the direction of application of the component forces on the bolt carrier, which occurs during in recoil of the bolt carrier. The forces acting on the bolt carrier during counter-recoil are shown in Fig. 6. These forces are cyclic in the case of multiple firing. The definition and detailed explanation of these forces have been presented in the documents [5, 16, 26, 27].

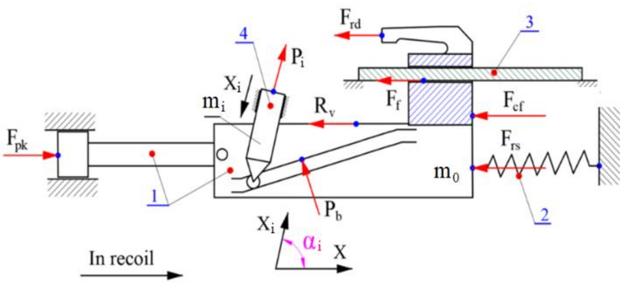

Fig. 5. Forces acting on the bolt carrier during recoil

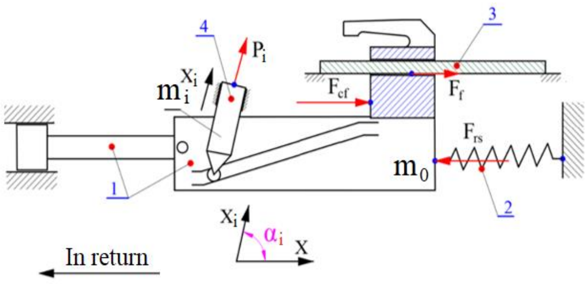

Fig. 6. Forces acting on the bolt carrier during return

Symbols in Fig. 5 and Fig. 6: 1. Bolt carrier and piston; 2. The return spring; 3. The guide rail on the receiver assembly; 4. The i-th working mechanism; F_{pk} – the force of the combustion gas pressure acting on the piston; P_i – generalized force effects on the i-th working mechanism; x – displacement of the bolt carrier relative to the gun body; x_i – displacement of the i-th working mechanism relative to the gun body; F_{rs} – the force of the return spring; F_{cf} – collision force between the bolt carrier and the gun body; F_{rd} – the force to remove a cartridge from the cartridge belt; R_v – cartridge case extraction force; P_b – resistance of the cartridge belt; F_f – friction force between the bolt carrier and the gun body.

3.3. Determination of gear ratios and transmission efficiency of mechanisms

The transmission ratio and efficiency of all mechanisms can be determined by analytical methods, mechanical models, or velocity graphical models for a series of positions of the mechanism. The gear ratio and transmission efficiency can be constant or variable depending on the cam profile at the linkage position. Two dynamic links must determine the gear ratio and efficiency of the PKMS machine gun. The gear ratio and efficiency of the link between the bolt carrier and the bolt is constant. The gear ratio and efficiency of the link between the bolt carrier and the feed lever depend on the distance traveled by the bolt carrier, see Fig. 7. In this study, the determination of gear ratio and transmission efficiency of the mechanisms is carried out by analytical method, the calculation is programmed on Matlab software.

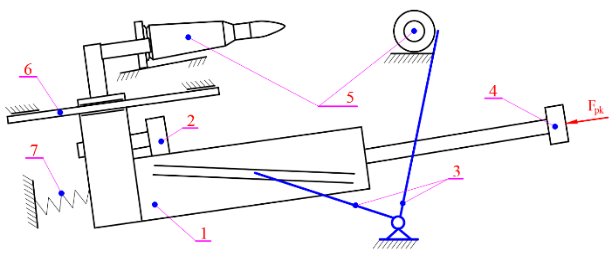

Fig. 7. Diagram of the automatic firing system of the PKMS machine gun (1. Bolt carrier; 2. Bolt; 3. Feed lever; 4. Piston; 5. Ammunition; 6. The slide line on the gun body; 7. Return spring)

a. The link between the bolt carrier and the bolt

The link diagram between the bolt carrier and the bolt is shown in Fig. 8.

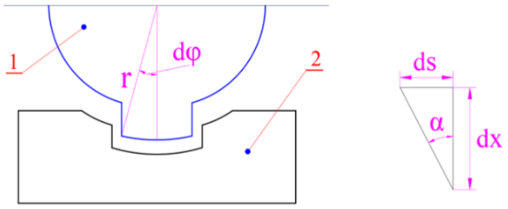

Fig. 8. The link diagram between the bolt carrier and the bolt (1. The bolt; 2. The bolt carrier)

According to the references [2, 3], the transmission ratio and efficiency from the bolt carrier to the bolt are determined according to the following equations:

$$k_1 = \frac{d\varphi}{dx} = \frac{tg\alpha}{r} = \frac{1}{0.16} = 6.25. \qquad (22)$$

$$\eta_1 = \frac{1 - f \cdot tg\alpha}{tg\alpha + 2f} tg\alpha = 0.654. \qquad (23)$$

Where: α – the tangent angle of the cam profile with the direction of motion of the bolt carrier. In the calculation, this angle is considered constant (α = 45°); f – coefficient of friction between the bolt carrier and the bolt, choose f = 0.15 (f = 0.15 ÷ 1.25).

b. The link between the bolt carrier and the feed lever

The link diagram between the bolt carrier and the feed lever is shown in Fig. 9.

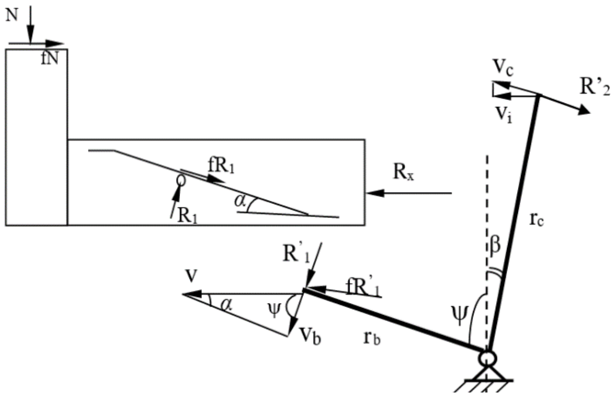

Fig. 9. The link diagram between the bolt carrier and the feed lever

On the reverse distance of the bolt carrier from x=0.02 to 0.12 (m), the radius of the cam groove on the bolt carrier acting on the feed lever is r_b. The angle in Fig. 9 is determined as follows:

When the bolt carrier is reversed:

$$\psi = \arccos\left(\cos\psi_{0l} - \frac{(x - 0.02) \cdot tg\alpha}{r_b}\right). \qquad (24)$$

When the bolt carrier is pushed up:

$$\psi = \arccos\left(\cos\psi_{0dl} - \frac{(x - 0.12) \cdot tg\alpha}{r_b'}\right). \qquad (25)$$

According to documents [2, 3], the equation for determining gear ratio and transmission efficiency is as follows:

The equation for determining gear ratio:

$$k_2 = \frac{v_i}{v} = \cos\beta \frac{r_c}{r_b} \frac{\sin\alpha}{\sin(\alpha + \psi)} \xi_{k2} \qquad (26)$$

The equation for determining transmission efficiency:

$$\eta_2 = \frac{R_2}{R_x} k_2 = \frac{\sin\psi(\cos\alpha - f\sin\alpha)\cos\beta}{\left[\sin\alpha(1 - f^2) + 2f\cos\alpha\right]} \frac{r_b}{r_c} k_2 \qquad (27)$$

Where, f – coefficient of friction between the feed lever and the bolt carrier; ξ_{k2} – the control variable is determined according to the following equation:

$$\xi_{k2} = \begin{cases} 0 \text{when} x < 0.02 or x > 0.12 \\ 1 \text{when} 0.02 \le x \le 0.12 \end{cases} \qquad (28)$$

4. RESULTS AND DISCUSSION

4.1. Problem solution

The numerical integration method was used to solve the system of equations (21). The 4th-order Runge-Kutta method was implemented in the Matlab R2022b programming environment. To obtain accurate results, the system of equations (21) is solved simultaneously with the system of interior ballistic equations in [3] and the system of gas chamber thermodynamic equations [15, 17].

Input parameters such as interior ballistic parameters and parameters of the structure were obtained from technical documents [28, 29]. The shape parameters of the part are measured directly on the gun in the equipment room. Some parameters are determined by SolidWorks design software such as coordinates of center of gravity, moment of inertia, point to apply force, etc.

Some typical results are shown from Fig. 10 to Fig. 13 . Where Fig. 10 shows the law of changing gas pressure in the barrel and the gas chamber; Fig. 11 shows the law of changing the bullet's velocity according to the length of the barrel; Fig. 12 shows the law of displacement and velocity of the bolt carrier over time; Fig. 13 shows the displacement law of the feed lever over time.

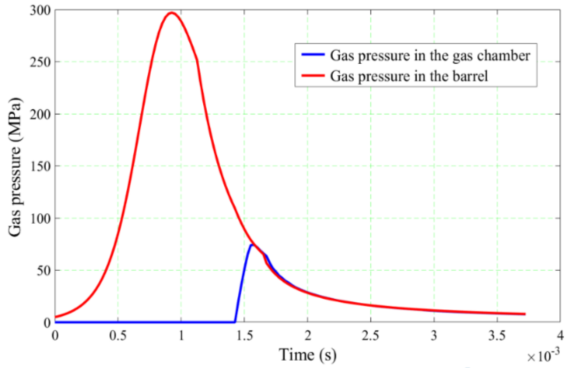

Fig. 10. Gas pressure in the barrel and the gas chamber

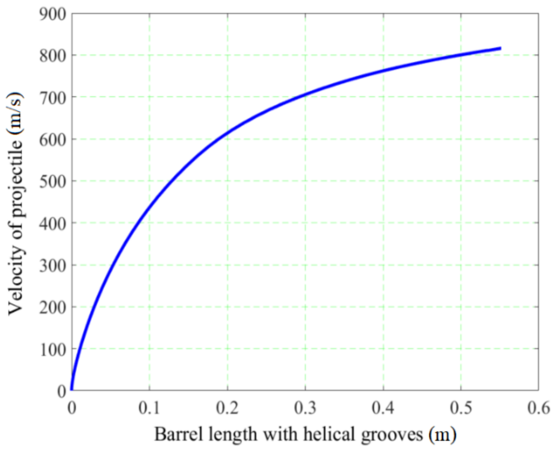

Fig. 11. The velocity of the projectile

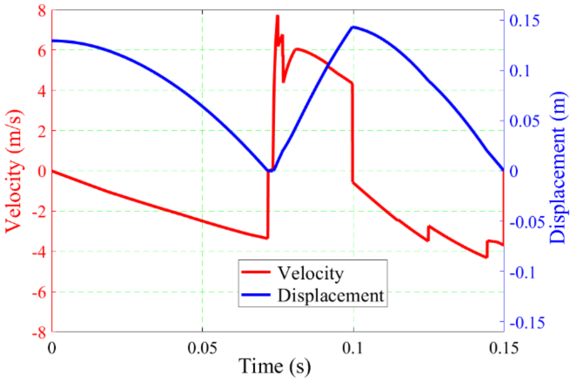

Fig. 12. The law of displacement and velocity of the bolt carrier

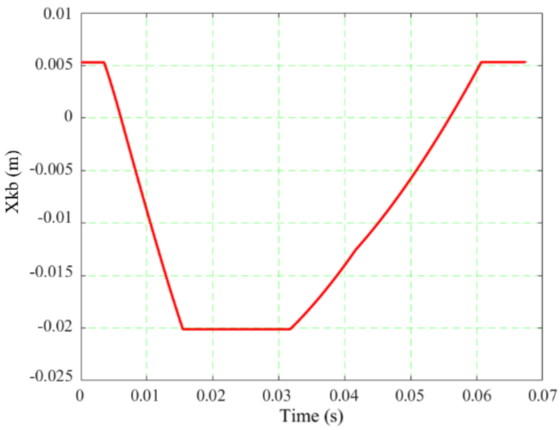

Fig. 13. The displacement law of the feed lever

4.2. Assessing the reliability of the established model

The reliable working of the automatic firing system is mainly evaluated based on the movement parameters of the base mechanism. Therefore, this study aims to determine the displacement and velocity of the base mechanism (the bolt carrier). The results obtained from the theoretical calculation are compared with the experimental results to verify the mathematical model.

In the experimental part of the study, the non-contact measurement technique was used by us. The movement of the bolt carrier is recorded with a high-speed camera, (position 4 in Fig. 14). The experimental diagram in this study is arranged as shown in Fig. 14.

Some pictures of the experimental layout are depicted in Fig. 15 and Fig. 16.

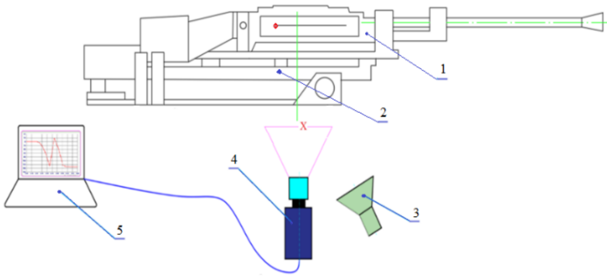

Fig. 14. Schematic of the experimental setup, (1. The PKMS machine gun; 2. Pedestal; 3. Lighting systems; 4. The high-speed camera; 5. The computer with data acquisition software)

The experiment was performed with the same procedure of 5 measurements. Measurements are made independently and under the same environmental conditions. Experimental conditions: temperature 20°C, humidity 65%, gun pedestal is placed stably and is not affected by external shock factors. Based on the recordings obtained from the High-Speed Camera, the displacement and velocity of the bolt carrier are determined through the data processing software. TeMA software was used to process the obtained data, [15, 16, 27, 30]. Some typical results of the experiments are presented in Table 1. Graphs of displacement and velocity over time at the first measurement are shown in Fig. 17 and Fig. 18. Where Fig. 17 shows the displacement of the bolt carrier while Fig. 18 shows the velocity of the bolt carrier.

Fig. 15. Test layout diagram

Fig. 16. The computer with data acquisition software

Table 1. The selected results of the experiment

Parameter	The 1st shot	The 2nd shot	The 3rd shot	The 4th shot	The 5th shot
The functional cycle time	0.0782 (s)	0.0815 (s)	0.0799 (s)	0.0811 (s)	0.0804 (s)
The time that the bolt carrier moves backward	0.0274 (s)	0.0286 (s)	0.0265 (s)	0.0283 (s)	0.0298 (s)
The time that the bolt carrier moves forward	0.0508 (s)	0.0529(s)	0.0534 (s)	0.0528 (s)	0.0506 (s)
The maximum velocity of the bolt carrier	7.474 (m/s)	7.148 (m/s)	7.136 (m/s)	7.355 (m/s)	7.043 (m/s)

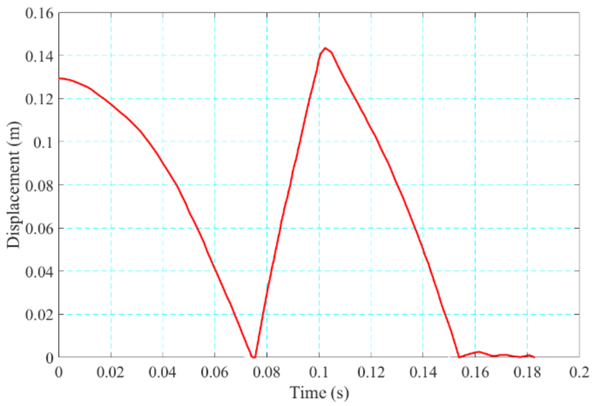

Fig. 17. Displacement of the bolt carrier

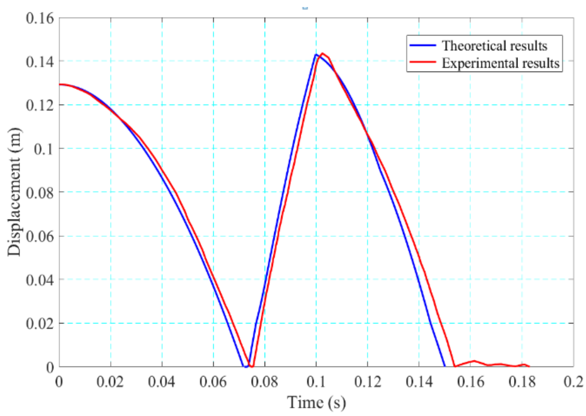

Fig. 19. Displacement graph of the bolt carrier

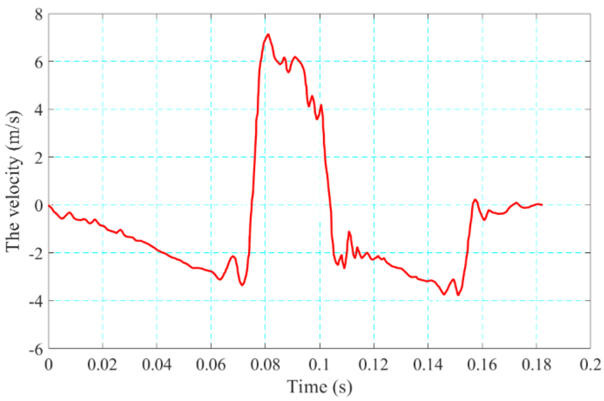

Fig. 18. The velocity of the bolt carrier

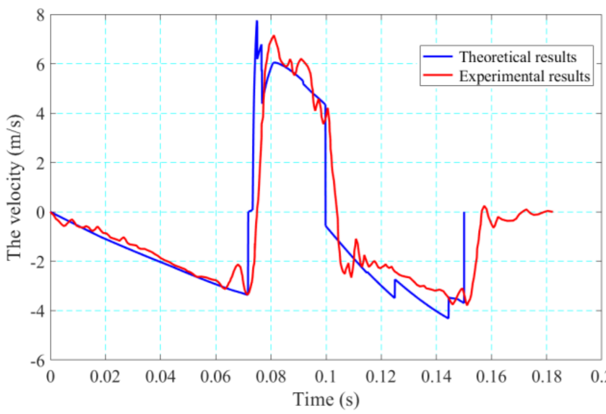

Fig. 20. Velocity graph of the bolt carrier

4.3. Discussions

The difference between theoretical calculation results and experimental results is shown in Fig. 19, Fig. 20, and Table 2.

The obtained results can be commented on as follows:

- The law of changing gas pressure in the barrel and the gas chamber is relatively consistent with the results already in the design documents [28].

According to the theoretical calculation, the maximum pressure value in the barrel is 288.46 (MPa); see Fig. 10, according to the manufacturer's design document is 299.2 (MPa), error of 3.72%.

- The accuracy and reliability of the theoretical model are confirmed when comparing the theoretical calculation results and the experimental results, see Fig. 19-20. The curve describing the displacement and the velocity of the bolt carrier according to the mathematical model and the results obtained from the experiment are relatively similar. The maximum error does not exceed 6.53%, Table 2.

- The time to make a shot according to the theoretical calculation is 0.0756 (s), equivalent to the theoretical fire rate of the gun of 794 (rds/min). The time to make a shot obtained from experimental results is 0.0802 (s), equivalent to a theoretical rate of fire of 748 (rds/min), error of 5.79%.

The analysis results show that the dynamic model of the automatic firing system of gas-operated automatic weapons is established to ensure reliability and can be used for further studies and surveys of the PKMS machine guns.

Table 2. Selected results of the solution

Parameter	Value		Error (%)
	Theoretical results	Experimental results	
The functional cycle time	0.0756 (s)	0.0802 (s)	6.08
The time that the bolt carrier moves backward	0.0263 (s)	0.0281 (s)	6.44
The time that the bolt carrier moves upward	0.0493 (s)	0.0521 (s)	5.89
The maximum velocity of the bolt carrier	7.7365 (m/s)	7.2313 (m/s)	6.53

5. CONCLUSION

This paper presents a method for setting up a dynamic model for the automatic firing system of a gas-operated automatic gun. The mathematical model is built based on Lagrange's equations of the second kind. The PKMS machine gun (Russia) was selected for the calculation and testing. With theoretical and experimental results obtained, we can get the following main conclusions:

- Calculation results according to the theoretical model are the displacement and velocity of the bolt carrier; the displacement of the feed lever. These parameters are the main concern of the dynamics problem of the automatic firing system.

- The mathematical model established in this study is relatively consistent with the actual gun model.

- The error of theoretical calculation results and experimental results do not exceed 6.53%. That proves the mathematical model is very good accuracy and reasonableness.

- This dynamic model applies to all types of automatic weapons. The results obtained from this study can be used in the design process to optimize the overall structure of the automatic firing system.

REFERENCES

[1] M. Macko, B.V. Vo, Q.A. Mai, Dynamics of Short Recoil-operated Weapon. *Problems of Mechatronics. Armament, Aviation, Safety Engineering*, 12(3), 2021: 9-26. https://doi.org/10.5604/01.3001.0015.2432

[2] P.H. Chuong, Textbook of structure and calculation on automatic firing system. *Military Technical Academy*, Hanoi, 1998. (in Vietnamese)

[3] L.A. Florio, Finite-Volume Modelling of System with Compressible Flow Propelled and Actuated Body Motion. *Applied Mathematical Modelling*, 33(8), 2009: 3360-3381. https://doi.org/10.1016/j.apm.2008.11.005

[4] D.V. Doan, V.V. Bien, M.A. Quang, N.M. Phu, A Study on Multi-Body Modeling and Vibration Analysis for Twin-Barrel Gun While Firing on Elastic Ground. *Applied Engineering Letters*, 8(1), 2023: 36-43. https://doi.org/10.18485/aeletters.2023.8.1.5

[5] D. Allsop, L. Popelinsky, J. Balla, V. Cech, S. Prochazka, J. Rosicky, Brasseys Essential Guide to Military Small Arms. *Brasseys,* London, United Kingdom, 1997.

[6] M. Fiser, L. Popelinsky, Small Arms. *University of Defence*, Brno, Czech Republic, 2007.

[7] M. Fiser, J. Balla, S. Prochazka, Automatic weapons – design and testing, Textbook. *Alexander University of Trencin*, Slovak Republic, 2007.

[8] M. Fiser, Design of small arms – impacts in mechanisms. *Military Academy, Brno, Czech Republic*, 1999.

[9] L. Popelinsky, Design of automatic weapons – calculation of functional diagram of automatic

weapon. *Military Academy*, Brno, Czech Republic, 2000.

[10] L. Popelinsky, J. Balla, High rate of fire automatic weapons – design and projecting, Textbook. *University of Defence*, Brno, Czech Republic, 2004.

[11] B.V. Vo, L. Dobsakova, N.V. Dung, D.P. Nguyen, T. D. Nguyen, M.P. Nguyen, A Study on Firing Stability of Howitzer Mounted on Wheeled Vehicles. *2023 International Conference on Military Technologies* (ICMT), Brno, Czech Republic, 2023, pp.1-7. https://doi.org/10.1109/ICMT58149.2023.10171322

[12] N.M. Mutafchiev, Methodology for Determining the Parameters of Gas Engine of Automatic Small Weapons. *International Scientific Conference "Defense Technology Forum 2015"*, Shumen, Bulgaria, 2015.

[13] L. Popelinsky, Gas Drive of Gas-Operated Automatic Weapons. *University of Defence, Brno*, Czech Republic, 1993.

[14] J. Balla, J. Horvath, Gas driver of machine gun. *International Conference on Military Technologies 2011*, Brno, Czech Republic, 2011.

[15] V.D. Tien, The Calculating Model of Impulse Force Diagram of Gas-Operated Automatic Weapons, Master Thesis. *University of Defence*, Brno, Czech Republic, 2013.

[16] D. Jevtic, D. Mickovic, S. Jaramaz, P. Elek, M. Markovic, S. Zivkovic, Modelling of Gas Parameters in the Cylinder of the Automatic Gun During Firing. *Thermal* Science, 24(6), 2020: 4135-4215. https://doi.org/10.2298/TSCI200118152J

[17] V.D. Tien, M. Macko, S. Procházka, V.V. Bien, Mathematical Model of a Gas-Operated Machine Gun. *Advances in Military Technology*, 17(1), 2022: 63–77. https://doi.org/10.3849/aimt.01449

[18] G.S. Karthik, K.J.Y. Kumar, V. Seshadri, Prediction of Performance Characteristics of Orifice Plate Assembly for Non-Standard Conditions Using CFD. *International Journal of Engineering and Technical Research (IJETR)*, 3(5), 2015: 162-167.

[19] A. Bagaskara, M.A. Moelyadi, CFD Based Prediction of Discharge Coefficient of Sonic Nozzle with Surface Roughness. *Journal of Physics: Conference Series*, 1005, 2018: 012010 https://doi.org/10.1088/1742-6596/1005/1/012010

[20] V. Horak, D.D. Linh, R. Vitek, S. Beer, Q.H. Mai, Prediction of the Air Gun Performance. *Advances in Military Technology*, 9(1), 2014: 31-44.

[21] V.D. Tien, S. Procházka, V. Horák, R. Vítek, P.B. Thanh, CFD Simulation of the Gas-Operated Weapon Drive Applied to the UK-59 Machine Gun. *Advances in Military Technology*, 17(2), 2022: 397–410. https://doi.org/10.3849/aimt.01743

[22] T.T. Hieu, U.S. Quyen, Using the experimental method to determine the dynamic parameters of the automatic weapon when firing. *Journal of Science and Technique*, No.123, 2008: 118-123.

[23] N.H. Lanh, N.V. Dung, V.X. Long, N.Q. Vinh, An experimental method for measuring the dynamics of automatic firearms when firing. *Journal of Science and Technique*, No.148, 2012: 175-182.

[24] D.D. Tran, M.P. Nguyen, V.B. Vo, D.P. Nguyen, M. Macko, M. Vitek, Analysis of gas flow losses in a gas-operated gun. *2023 International Conference on Military Technologies (ICMT)*, 23-26 May 2023, Brno, Czech Republic, pp.1-7. https://doi.org/10.1109/ICMT58149.2023.10171337

[25] A.A. Shabana, Dynamics of multibody systems. *Cambridge University Press*, Cambridge, United Kingdom, 2020.

[26] J. Balla, Contribution to Determining of Load Generated by Shooting from Automatic Weapons. *2019 International Conference on Military Technologies (ICMT),* 30-31 May 2019, Brno, Czech Republic, pp.1-6.

[27] J. Balla, V.D. Nguyen, Z. Krist, M.P. Nguyen, V.B. Vo, Study Effects of Shock Absorbers Parameters to Recoil of Automatic Weapons. *2021 International Conference on Military Technologies (ICMT)*, 8-11 June 2021, Brno, Czech Republic, pp.1-6. https://doi.org/10.1109/ICMT52455.2021.9502825

[28] P.N. Thieu, K.Đ. Tuy, Typical armament of synthetic weapons, part 5. *Military Technical Academy*, Hanoi, 2004. (in Vietnamese)

[29] J. Balla, L. Popelisky, Z. Krist, Theory of High Rate of Fire Automatic Weapon with Together Bound Barrels and Breeches. *WSEAS Transactions on Applied and Theoretical Mechanics*, 5(1), 2010: 71-80.

[30] S. Beer, L. Jedlicka, B. Plihal, Barrel Weapons Interior Ballistics. *University of Defence*, Brno, Czech Republic, 2004. (in Czech).